Wadi Alshatti University Journal of Pure and Applied Sciences

مجلة جامعة وادي الشاطئ للعلوم البحتة والتطبيقية

Volume 4, No. 1, January-June 2026 Online ISSN: 3006-0877 المجلد 4، الاصدار 1، يناير - يونيو 2026

RESEARCH ARTICLE **PHYSICS**

Effect of Mn-Site Doping on the Magnetic Properties of the $La_{2/3}Sr_{1/3}Mn_{1-x}In_xO_3$ Manganite Perovskite

Ramadan E. Shaiboub[1*], Ali Agail Hamed[2]

[1]Physics Department, Faculty of Education, Nalut University, Nalut, Libya
[2]Computer Science Department, Faculty of Science, Wadi Alshatti University, Brack, Libya

ARTICLE HISTORY
Received 19 July 2025
Revised 20 December 2025
Accepted 20 January 2026
Online 26 January 2026

KEYWORDS
Perovskite;
Magnetic Susceptibility;
Magnetic properties;
Magnetoresistance;
Curie temperature.

ABSTRACT

The substitution of Mn with a low concentration of In ($x \leq 0.20$) in the magnetoresistance compound $La_{2/3}Sr_{1/3}Mn_{1-x}In_xO_3$ has been investigated. Magnetic properties were analyzed using AC magnetic susceptibility and DC electrical resistance measurements. The metal-to-insulator transition temperature (Tp)decreased from 365 K to 245K as the level of In doping increased, indicating a loss of ferromagnetic order. Similarly, the Curie temperature (Tc) of each sample shifted to lower values with higher In content. X-ray diffraction (XRD) analysis revealed a single-phase perovskite rhombohedral structure. Surface morphology and microstructural analysis using scanning electron microscopy (SEM) indicated that withan increase in Indium concentration up to x= 0.20, grain size diminished significantly, reducing from 15 µm to 2 µm, along with noticeable grain agglomeration.

تأثير التشويب في موقع المنغنيز على الخواص المغناطيسية لبيروفسكايت المنغنيت $La_{2/3}Sr_{1/3}Mn_{1-x}In_xO_3$

رمضان ابراهيم شيبوب[1*]،علي عقيل حامد[2]

الكلمات المفتاحية
بيروفسكايت
الحساسية المغناطيسية
الخواص المغناطيسية
المقاومة المغناطيسية
درجة حرارة كوري

الملخص

تمت دراسة استبدال المنغنيز بتركيز منخفض من الإنديوم ($x \leq 0.20$) في مركب المقاومة المغناطيسية $La_{2/3}Sr_{1/3}Mn_{1-x}In_xO_3$. وتم تحليل الخصائص المغناطيسية باستخدام قياسات الحساسية المغناطيسية للتيار المتردد والمقاومة الكهربائية للتيار المستمر. انخفضت درجة حرارة التحول من المعدن إلى العازل (Tp) من 365 كلفن إلى 245 كلفن مع زيادة مستوى تطعيم الإنديوم، مما يشير إلى فقدان الترتيب المغناطيسي الحديدي. وبالمثل، انخفضت درجة حرارة كوري (Tc) لكل عينة مع زيادة محتوى الإنديوم. وكشف تحليل حيود الأشعة السينية (XRD) عن بنية بيروفسكايت معينية الأوجه أحادية الطور. وأشارت دراسة مورفولوجيا السطح وتحليل البنية المجهرية باستخدام المجهر الإلكتروني الماسح (SEM) إلى أنه مع زيادة تركيز الإنديوم حتى $x = 0.20$، انخفض حجم الحبيبات بشكل ملحوظ، من 15 ميكرومتر إلى 2 ميكرومتر، مصحوبًا بتكتل ملحوظ للحبيبات.

INTRODUCTION

Perovskite manganites, represented by the formula R1-xAxMnO3 (where R denotes a trivalent rare-earth ion and A represents a divalent ion such as Ca,Sr, Ba, or Pb), have garnered significant scientific and technological attention due to their colossal magnetoresistance (CMR) effect. This property holds promising potential for applications in magnetic sensors and read heads. Among these compounds, the doped mixed-valent La0.67Sr0.33MnO3, belonging to the perovskite family, exhibits intriguing electrical and magneto-transport behaviors, particularly the CMR phenomenon. The CMR effect, first explained by Zener through the double exchange (DE) mechanism, occurs as part of a phase transition from a paramagnetic insulator state at higher temperatures to a ferromagnetic metallic state at lower temperatures (Tp) [1–3].

Research [4–6] has revealed that the magnetism of Mn in manganites exhibiting CMR is influenced not only by the ferromagnetic DE interaction but also by the superexchange (SE) interaction mediated via O ions bridging Mn ions. It is established that Mn3+-O2--Mn4+ interactions lead to ferromagnetism, whereas both Mn3+-O2--Mn3+ and Mn4+-O2--Mn4+ interactions result in antiferromagnetism. Furthermore, these interactions are further complicated by the presence of dopants, which introduce additional complex interactions between the central Mn ions and the dopant ions [7]. These intricacies significantly impact the magnetic behavior of the system [8–10].

Complex magnetic behavior often emerges in mixed-valence manganites synthesized through full doping, where a delicate interplay exists between double exchange (DE) and superexchange (SE) interactions. The fundamental magnetic and transport properties of these materials are highly sensitive to both the geometry of the Mn–O–Mn network and the Mn^{3+}/Mn^{4+} ratio. While extensive research has focused on

*Corresponding author
https://doi.org/10.63318/waujpasv4i1_11

substituting La with other rare-earth elements, comparatively fewer studies have examined doping at the Mn site. Considering the pivotal role of Mn in the conduction mechanism, partial substitution with other transition metals can provide deeper insights into the underlying physical processes [11-18]. In this work, we investigate the effects of indium (In) doping on the structural, electrical, and magnetic properties of $La_{0.67}Sr_{0.33}MnO_3$. Detailed analyses of electrical resistivit]y, magnetic behavior, and microstructural characteristics reveal the influence of In incorporation on the double exchange mechanism and overall magnetic ordering.

The importance of this article lies in improving the thermoelectric properties of solar Photovoltaic cells [19-24], which are expected to play a pivotal role in the transition towards renewable and environmentally friendly energies, as photovoltaic solar cells are projected to exceed 50% of the total installed renewable energies worldwide by 2025 [25-38].

EXPERIMENTAL AND METHODOLOGY

Polycrystalline compounds with the composition $La_{0.67}Sr_{0.33}Mn_{1-x}In_xO_3$ were synthesized using the solid-state reaction method. High-purity powders of La_2O_3, $SrCO_3$, MnO_2, and In_2O_3 (greater than 99.9%) were thoroughly mixed and ball-milled in acetone for 24 hours. The mixture was then dried in an oven at 110 ºC for 12 hours to obtain a fine and homogeneous powder. The prepared powder, corresponding to the target composition $La_{0.67}Sr_{0.33}Mn_{1-x}In_xO_3$, was calcined in air at 900 ºC for 12 hours, with a heating rate of 3ºC/min. Following calcination, The material was ground for 20 minutes and subsequently sieved through a 45 µm sieve. Following this, pellets were fabricated by pressing 1.2 g of the powder under a hydraulic press with a force of 30 kN, resulting in discs measuring 10 to 12 mm in diameter. These pellets were sintered at 1300 ºC for 24 hours, employing a controlled heating rate of 2 ºC/min. After the sintering process, the samples were allowed to cool naturally to room temperature.

Sample characterization was conducted using an X-ray diffractometer (XRD, Philips PW1830) equipped with Cu Kα radiation. The scanning angles (θ) were set between 20º and 80º. Electrical resistance measurements were carried out via the conventional four-probe technique over a temperature range of 20 K to 300 K in the absence of magnetic fields. The instrumentation for these measurements included a Lake Shore 330 auto-tuning temperature controller, a Keithley 128 sensitive digital voltmeter, a Keithley 224 programmable current source, a Keithley 7001 switch system, and automated PC-based control software. Additionally, AC susceptibility measurements were performed using a Lake Shore Cryotronics AC susceptometer (Model 7000) across a temperature range of 30 K to 300 K. Measurements were taken under an alternating magnetic field ranging from 0.1 Oe to 10 Oe at a frequency of 125 Hz.

RESULTS AND DISCUSSION

The samples of LSMInO were characterized with the x-ray diffractometer using (CuKα) x-ray in order to see the structure of the samples with λ=1.54056 Å. Figure 1, shows the XRD spectrum of each sample at 2θ ranged from 20º-80º. The samples have similar single-phase behavior and exhibited almost the same peaks reveals similar pattern to undoped sample. All the samples are in rhombhedral form of perovskite structure. Based on the XRD analysis, the lattice parameters and unit-cell volumes were calculated using the Chekcell program, as summarized in Table 1. A noticeable decrease in unit-cell volume is observed with increasing doping concentration, reducing from 116.66 Å³ to 114.49 Å³ compared to the undoped sample. This contraction in volume is consistent with findings reported by other researchers.

All samples maintain a rhombohedral perovskite structure. The substitution of In ions at the Mn sites, particularly at higher doping levels, results in a reduction of the unit-cell volume in LSMInO manganites, the overall reduction in unit cell volume with increased x could be due to other structural adjustments or the interplay of different ionic sizes [39,40].

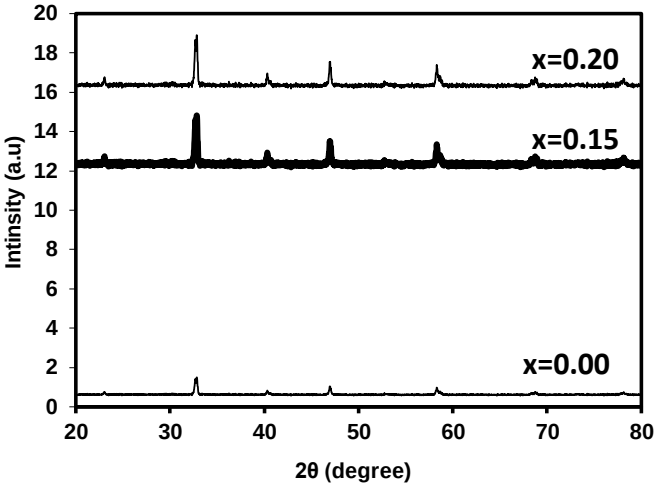

Figure 1: XRD spectra for the LSMInO samples

Table 1: Lattice parameters, a=b=c and unit-cell volume of LSMInO samples

Concentration (In)	a (Å)	V(Å)³
0.00	5.471	116.66
0.15	5.460	114.80
0.20	5.458	114.49

The resistance versus temperature curves for (LSMInO) in the absence of an external magnetic field are presented in Figure 2, comparing undoped samples with those doped with indium content (≤ 0.20). The undoped sample exhibits a metal-insulator transition, with maximum resistance observed at Tp (365 K).

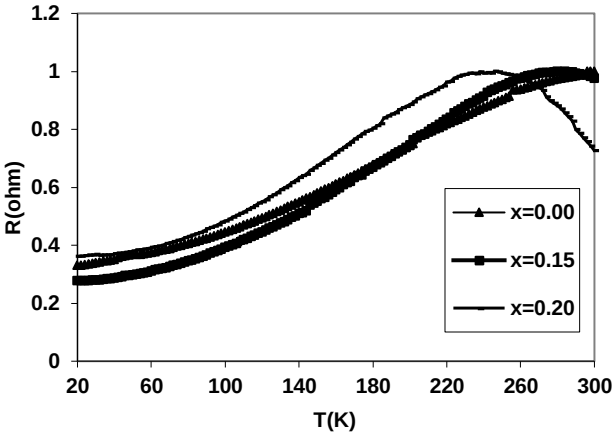

Figure 2: The relationship between resistance and temperature for LSMInO samples

However, this is not shown in the figure due to the measurement apparatus being limited to a range of up to 300 K. As the indium concentration increases to 0.20%, the resistance decreases, and the Tp shifts to a lower temperature, dropping from 365 K to 245 K. Nonetheless, all samples display metallic behavior below Tp.

As the Indium content increases, both Tc and Tp decrease, indicating a general weakening of the ferromagnetic double

exchange (DE) interaction between In^{3+} and M^{3+} in the formation of In^{3+}-O^{2-}-M^{3+}.Simultaneously, there is an increasing influence of antiferromagnetic interactions resulting from superexchange. The magnetic and electrical phase diagram of the LSMInO samples is constructed by plotting Tp and Tc as functions of the Indium content, as demonstrated in Figure 3. When the Indium concentration reaches x = 0.20, both Tc and Tp begin to decrease consistently. Tp exhibits a more significant decrease compared to Tc. As a result, in the region between Tc and Tp, the PMM state transitions to the FMI state when the doping level reaches x = 0.20.

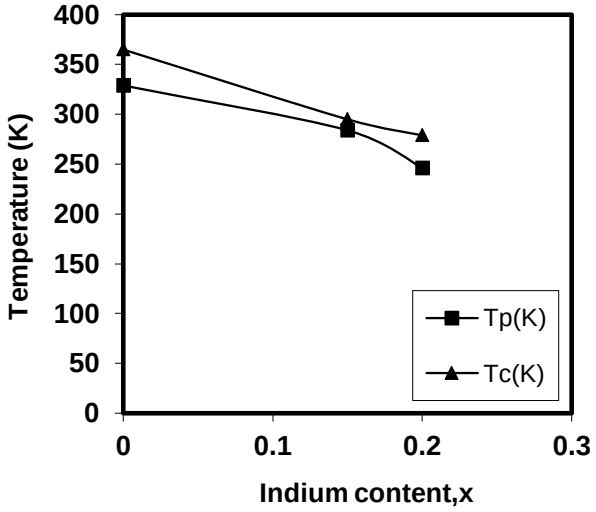

Figure 3: The variation of T_c and T_p with Indium content (x) in the samples

The temperature range of 30–300 K measured at a frequency of 125 Hz, along with susceptibility data at 5 Oe, is illustrated in Figure 4. For the undoped sample (x = 0.00), the Curie temperature (Tc) was found to be approximately 365 K, exceeding the operational range of the measurement system, which was limited to 300 K;hence, it is not shown in the figure. During the cooling process, a phase transition from paramagnetic to ferromagnetic was observed for x = 0.15 and x = 0.20, with corresponding Tc values of 287 K and 279 K.

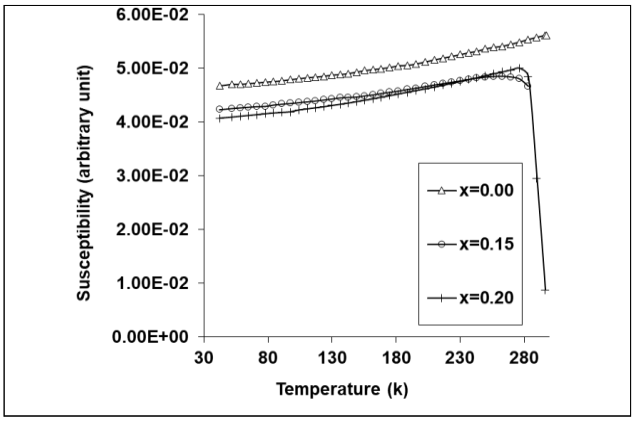

Figure 4: The AC susceptibility of LSMInO samples, measured at 5 Oe

These results demonstrate that ferromagnetic materials transition to a paramagnetic state as the temperature surpasses Tc. Additionally, the ferromagnetic characteristics of the sample diminish as the indium content increases. This occurs due to the progressive disruption of Mn3+-O2--Mn4+ bonds, leading to the localization of eg electrons in Mn3+ ions. As a result, increasing levels of indium weaken the double exchange interaction within the sample, thereby reducing the ferromagnetic alignment of electron spins at lower temperatures.

The microstructure of LSMInO samples with (x≤0.20) are shown in figure 5(a, b and c). The purpose of SEM analysis is to determine the physical parameters of grain size, grain growth and porosity. The microstructures of all the samples were investigated at the magnification of 2000X. The undoped sample with x=0.00 shows the grain size with an average of 15 µm. The samples show some pores and the surface becomes fused. As Indium concentration increases to x=0.20, the grain becomes smaller of about 2 µm with grain agglomeration.

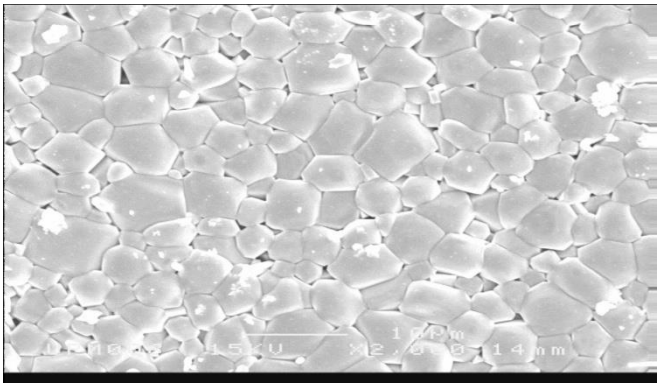

Figure 5a: SEM image of the microstructure of LSMInO sample (x=0.00)

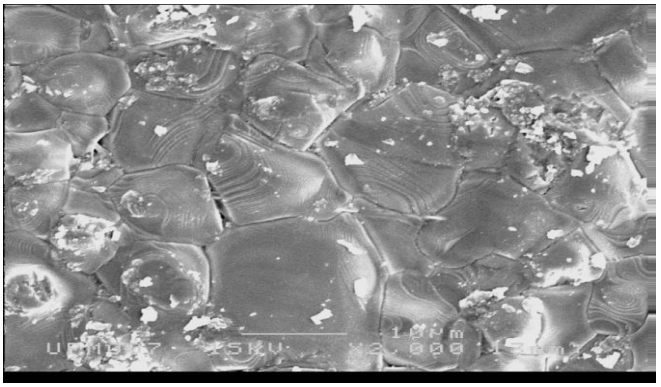

Figure 5b: SEM image of the microstructure of LSMInO sample (x=0.15)

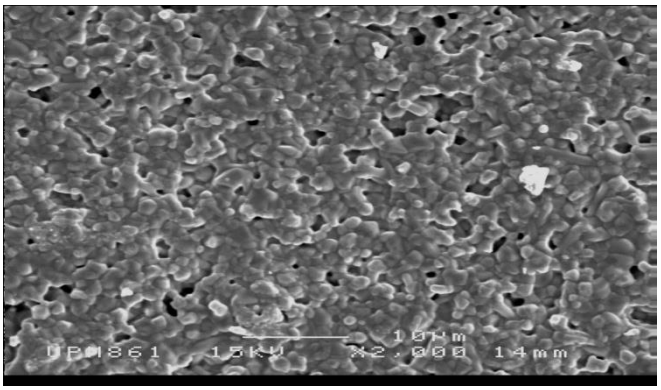

Figure 5c: SEM image of the microstructure of LSMInO sample (x=0.20)

CONCLUSION

In this study, the impact of Mn substitution in $La_{2/3}Sr_{1/3}Mn_{1-x}In_xO_3$samples with x= 0.00, 0.15, and 0.20 reveals a competition between double exchange (DE) ferromagnetism and superexchange antiferromagnetism. This interaction results in a reduction of the Curie temperature (Tc) as the doping concentration increases. All samples display a shared characteristic of transitioning from a paramagnetic (PM) state to a ferromagnetic (FM) state. Furthermore, as doping levels rise, the metal-insulator transition temperature decreases from above 300 K for x = 0.00 to lower values. Additionally, an expansion in unit-cell volume is observed with increasing x, attributed to the larger ionic size of In^{3+}. The system also exhibits a decrease in unit cell volume as x increases could result from other structural modifications or the interaction between varying ionic sizes. This study primarily analyzed indium concentrations up to x = 0.20. However, extending the scope to include higher doping levels may offer a more thorough insight into their influence on magnetic properties and structural phase transitions. Also, may be sophisticated microscopy methods like transmission electron microscopy (TEM) and atomic force microscopy (AFM) to conduct in-depth microstructural analysis. These techniques can uncover valuable details about grain boundary features and their influence on magnetic properties.

Author Contributions: "Agail: Conceptualization and methodology, writing—original draft preparation, review, and editing. **Shaiboub**: Data collection, analysis of results, and discussion. Both authors have read and agreed to the published version of the manuscript."

Funding: "This research received no external funding."

Acknowledgements: " We extend our sincere thanks and appreciation to the Ministry of Higher Education and Scientific Research in Libya for its financial support, and to UPM University Malaysia for its cooperation and logistical support, which contributed to the success of this project. "

Conflicts of Interest: "The authors declare that they have no conflict of interest."

Data Availability Statement: "No data were used to support this study."

REFERENCES

[1] E. Dagotto. "Complexity in strongly correlated electronic systems." *Science*, vol. 309, pp. 257–262, 2010. https://doi.org/10.1126/science.1107559

[2] Y. Tokura, and N. Nagaosa. "Orbital physics in transition-metal oxides." *Nature Materials*, vol. 11, no. 7, pp. 567584, 2012. https://doi.org/10.1126/science.288.5465.462

[3] M. Bibes, and A. Barthélémy. "Oxide spintronics." *IEEE Transactions on Electron Devices*, vol. 54, no. 5, pp. 1003–1023, 2013. https://doi.org/10.1109/TED.2007.894366

[4] M. Smari. "Dy-doped $La_{0.51}Sr_{0.49}MnO_3$ nanoparticles: Tuning structural and magnetocaloric properties via sol-gel synthesis for energy-efficient applications." *Nano Trends*, vol. 9, p. 100069, 2025. https://doi.org/10.1016/j.nwnano. 2024.100069

[5] P. Namboothiri. "Impact of Mg substitution in LaMnO3 manganites on their structural integrity and magnetic behavior." *RSC Advances*, vol. 15, pp. 8561-8571, 2025. https://doi.org/10.1039/D4RA08238A

[6] L. Ali. "Tuning of the band gap and suppression of metallic phase by Ca doping in $La_{1-x}Ca_xMnO_3$ manganite nanoparticles." *Scientific Reports*, vol. 15, p. 44062, 2025. https://doi.org/10.1038/s41598-024-80429-8

[7] C. Zhou, and R. Li. "Magnetocaloric effect in $La_{0.7}Sr_{0.3}Mn_{0.95}Ni_{0.05}O_3$ manganite via mean field theory." *Journal of Material Science and Technology Research*, 2025. https://doi.org/10.31875/2410-4701.2025.12.02

[8] M. Tata. "Synthesis, structure, morphology, magnetism, and magnetocaloric effect studies of $La_{0.7}Sr_{0.3}Mn_{1-x}Fe_xO_3$ perovskite nanoparticles." *Journal of Alloys and Compounds*, vol. 958, P. 170454, 2023. https://doi.org/10.1016/j.jallcom.2023.170454

[9] C. Zhou, et al. "Molybdenum-doped $La_{0.7}Sr_{0.3}MnO_3$ nanoparticles: Tuning magnetic and heating properties for magnetic hyperthermia." *RSC Advances*, 2026. https://doi.org/10.1039/D5RA08765A

[10] J. Li. "Magnetic and electronic properties of La-doped hexagonal 4H-SrMnO3." *Chinese Physics B*, vol. 33, no. 1, 017502, 2024. https://doi.org/10.1088/1674-1056/acf995

[11] F. Azim. "Study of magnetic and magnetocaloric properties of calcium doped $La_{0.97-x}Ca_xHo_{0.03}MnO_3$ compound. MRS Advances, 9, 790-796, 2024. https://doi.org/10.1557/s43580-024-00810-7

[12] M. Ghozza, I. Yahia, and M. Hussien. "Structure, magnetic, and photocatalysis of $La_{0.7}Sr_{0.3}MO_3$ (M = Mn, Co, Fe) perovskite nanoparticles." *Environmental Science and Pollution Research*, vol. 30, pp. 61106–61122, 2023. https://doi.org/10.1007/s11356-023-26411-9

[13] X. Jin, et al. "Influence of high-pressure heat treatment on magnetic property and phase transition critical behavior in $La_{0.75}Sr_{0.25}Mn_{1-x}Co_xO_3$." *Results in Physics*, vol. 57, p. 107392, 2024. https://doi.org/10.1016/j.rinp.2024.107392

[14] X. Jin, et al. "Role of nickel doping on magnetocaloric properties of $La_{0.7}Sr_{0.3}Mn_{1-x}Ni_xO_3$ manganites." *Journal of Materials Science: Materials in Electronics*, vol. 2, p. 15000–15010, 2021. https://doi.org/10.1007/s10854-021-05702-2

[15] J. Hala, et al. "Performance investigation of multilayer-layers solar cell based in ZnS-CZTSSe." *Solar Energy*, vol. 291, p. 113410, 2025. https://doi.org/10.1016/j.solener. 2025.113410

[16] P. Santos, L. Azevedo, P. Freitas, P. Araujo. "Magnetic interactions in $La_{0.7}Sr_{0.3}Mn_{1-x}Me_xO_3$ (Me = Ga, Fe, Cr) manganites." *Journal of Magnetism and Magnetic Materials*, vol. 382, pp. 253–260, 2015. https://doi.org/10.1016/j.jmmm.2015.06.046

[17] S. Yazdi, et al. "Magnetotransport and magnetoelastic effects in Co-doped $La_{0.7}Sr_{0.3}MnO_3$ nanocrystalline perovskites." *Journal of Magnetism and Magnetic Materials*, vol. 322, pp. 3451–3456, 2010. https://doi.org/10.1016/j.jmmm.2010.05.046

[18] X. Jin. "Influence of high-pressure heat treatment on magnetic property and phase transition critical behavior in $La_{0.75}Sr_{0.25}Mn_{1-x}Co_xO_3$ (x = 0, 0.1, 0.2)." *Results in Physics*, vol. 57, p. 107392, 2024. https://doi.org/10.1016/j.rinp.2024.107392

[19] K. Moumani. "Management of sustainable development in the light of Arab and international cooperation, a case study of the Arab vision of management of sustainable development." *Wadi Alshatti University Journal of Pure and Applied Sciences*, vol. 1, no. 1, pp. 1-8, 2023. https://doi.org/10.63318/waujpasv1i1_01

[20] H. El-Khozondar, et al. "Simulation results for the PV cell based on the photonic crystal." *Optik*, vol. 270, 2022, p. 169966, https://doi.org/10.1016/j.ijleo.2022.169966

[21] R. El-Khozondar, et al. "Efficiency improvement of Ag-doped CdSe quantum dot sensitized solar cells." *2023 8th International Engineering Conference on Renewable Energy & Sustainability (ieCRES)*, Gaza, Palestine, State of, 2023, pp. 1-5, https://doi.org/10.1109/ieCRES57315.2023.10209498

[22] A. Aqila, et al. "Design of hybrid renewable energy system (PV/Wind/Battery) under real climatic and operational conditions to meet full load of the residential sector: A case study of a house in Samno village– southern region of Libya. *Wadi Alshatti University Journal of Pure and Applied Sciences*, vol. 3, no. 1, pp. 168-181, 2025. https://doi.org/10.63318/ waujpasv3i1_23

[23] K. Amer, et al. "Economic-environmental-energetic (3e) analysis of photovoltaic solar energy systems: Case study of Mechanical & Renewable Energy Engineering Departments at Wadi AlShatti University." *Wadi Alshatti University Journal of Pure and Applied Sciences*, vol. 3, no. 1, pp. 51-58, 2025. https://doi.org/10.63318/ waujpasv3i1_09

[24] H. Abdulgader, et al. "Mitigation of dust impact on solar photovoltaics performance considering libyan climate zone: A

review." *Wadi Alshatti University Journal of Pure and Applied Sciences*, vol. 1, no. 1, pp. 22-27, 2025. https://www.waujpas.com/index.php/journal/article/view/7

[25] E. Hala, et al. "Economic and environmental implications of solar energy street lighting in urban regions: A case study." *Wadi Alshatti University Journal of Pure and Applied Sciences*, vol. 3, no. 1, pp. 142-151, 2025. https://doi.org/10.63318/waujpasv3i1_21

[26] E. Salim, A. Abubaker, and B. Ahmed. "A brief overview of hybrid renewable energy systems and analysis of integration of isolated hybrid PV solar system with pumped hydropower storage for Brack city - Libya." *Wadi Alshatti University Journal of Pure and Applied Sciences*, vol. 3, no. 1, pp. 152-167, 2025. https://doi.org/10.63318/ waujpasv3i1_22

[27] M. Al-Maghalseh. "The environmental impact and societal conditions of PV power plants: a case study of Jericho gate-Palestine Stat Of." *Wadi Alshatti University Journal of Pure and Applied Sciences*, vol. 3, no. 2, pp. 16-31, 2025. https://doi.org/10.63318/waujpasv3i2_03

[28] A. Al-Mathnani, A. Mohammed, S. Al-Hashmi, and E. Geepalla. "Control and modification of 12-pulse static compensator with PV cell using new control algorithm." *Wadi Alshatti University Journal of Pure and Applied Sciences*, vol. 3, no. 1, pp. 30-34, 2025. https://doi.org/10.63318/waujpasv3i1_06

[29] D. Albuzia, A. Ali, M. Mohmed, and A. Hafez. "reliable and robust optimal interleaved boost converter interfacing photovoltaic generator." *Wadi Alshatti University Journal of Pure and Applied Sciences*, vol. 3, no. 2, pp. 192-201, 2025. https://doi.org/10.63318/waujpasv3i2_24

[30] A. Alkhazmi, et al. "Design and analysis of PV solar street lighting systems in remote areas: A case study." *Wadi Alshatti University Journal of Pure and Applied Sciences*, vol. 4, no. 1, pp. 1-14, 2026. https://doi.org/10.63318/ waujpasv4i1_01

[31] I. Latiwash. "Performance analysis and sizing optimization of a utility scale stand-alone renewable energy PV/Battery storage system for urban zones." *University of Zawia Journal of Engineering Sciences and Technology*, vol. 3, no. 2, pp. 261–275, 2025. https://doi.org/10.26629/uzjest. 2025.21

[32] L. Ben Dalla, O. Karal, M. EL-Sseid, and A. Alsharif. "An IoT-enabled, THD-Based fault detection and predictive maintenance framework for solar PV systems in harsh climates: integrating dft and machine learning for enhanced performance and resilience." *Wadi Alshatti University Journal of Pure and Applied Sciences*, vol. 4, no. 1, pp. 41-55, 2025. https://doi.org/10.63318/waujpasv4i1_ 05

[33] B. Ahmed, N. Fathi, H. El-Khozondar, and M. Khaleel. "Optimal Design of Hybrid Renewable Energy System (PV/Wind/PHS) Under Multiple Constraints of Connection to the Electricity Grid: A Case Study." *Wadi Alshatti University Journal of Pure and Applied Sciences*, vol. 4, no. 1, pp. 83-93, 2026. https://doi.org/10.63318/waujpasv4i1_ 09

[34] I. Imbayah, et al. "Design of a PV Solar-Covered Parking System for the College of Renewable Energy Tajoura, Libya: A PVsyst-Based Performance Analysis." *University of Zawia Journal of Engineering Sciences and Technology*, vol. 3, no. 2, pp. 288–307, 2025. https://doi.org/10.26629/uzjest. 2025.23

[35] A. Aqila, et al. "Design and Analysis of a (PV/Wind/Battery) Hybrid Renewable Energy System for Residential buildings under real time conditions." *Engineering for Palestine Conference*, Palestine Polytechnic University, Hebron, Palestine, 29–30 September 2025. https://www.researchgate.net/publication/396910534

[36] J. Hala, et al. "Sustainable street lighting in Gaza: Solar energy solutions for main street." *Energy 360*, vol. 4, p. 100042, 2025. https://doi.org/10.1016/j.energ.2025.100042

[37] A. Aqila, A. Abubaker, and N. Fathi. "Design of a Hybrid Renewable Energy System to Meet Housing Thermal Loads: Performance Evaluation Under Real Conditions of a House in Samno Region, Libya." *Wadi Alshatti University Journal of Pure and Applied Sciences*, vol. 3, no. 2, pp. 179-191, 2025. https://doi.org/10.63318/waujpasv3i2_23

[38] E. Almhdi, and G. Miskeen. "Power and Carbon Footprint Evaluation and Optimization in Transitioning Data Centres." *Wadi Alshatti University Journal of Pure and Applied Sciences*, vol. 3, no. 2, pp. 221-229, 2025 . https://doi.org/10.63318/waujpasv3i2_28

[39] M. Mohamed, et al. "Structural, optical, magnetic, and dielectric investigations of pure and Co-doped $La_{0.67}Sr_{0.33}Mn_{1-x-y}Zn_xCo_yO_3$ manganites with ($0.00 < x + y < 0.20$)." *Crystals*, vol. 14, no. 11, pp. 981, 2024. https://doi.org/10.3390/cryst14110981

[40] M. Al-Shahumi, et al. "Synthesis, structure, morphology, magnetism, and magnetocaloric-effect studies of $La_{0.7}Sr_{0.3}Mn_{1-x}Fe_xO_3$ perovskite nanoparticles." *Journal of Alloys and Compounds*, vol. 958, p. 170454, 2023. https://doi.org/10.1016/j.jallcom.2023.170454